DEPT. OF MATH., UNIVERSITY OF OSLO
RESEARCH REPORT IN MECHANICS, No. 1
ISSN 0801-9940 December 2012
(Revised July 2014)

TRIALS WITH A SIMPLIFIED METHOD FOR BUCKLING AND ULTIMATE STRENGTH ANALYSIS OF COMPOSITE PLATES

by

Qiao Jie Yang, Brian Hayman and Harald Osnes

Mechanics Division, Department of Mathematics
University of Oslo, Norway

Abstract: The work presented here concerns the ultimate strength of simply supported, square plates subjected to uniaxial in-plane compressive load. Plates having a range of thicknesses and initial geometric imperfections have been investigated. Several models based on first order shear deformation theory combined with assumption of small deflections are presented. In the simplest models, fulfilment of a failure criterion at any position in a ply leads to degradation of corresponding stiffness properties throughout that ply. The approach is shown to give reasonable but somewhat conservative estimates of ultimate loads for the thicker plates considered, while for the thinner plates, neglect of the post-buckling behaviour causes low accuracy of the results. A slightly more detailed model in which the plate is divided into nine regions and the stiffness degradation is limited to a single region of a failed ply gives marginally better results in some of the cases analysed. However, to realise the full potential of this model it will be necessary to use a large deflection plate theory.

Keywords: Composite plates; Ultimate strength; Buckling; Instantaneous material degradation.

CONTENTS

1 INTRODUCTION 2
1.1 Background 2
1.2 The Present Study 3
2 PROGRESSIVE FAILURE MODELS 5
2.1 Overall Description 5
2.2 Tsai-Wu Failure Criterion 5
2.3 Hashin and Rotem Failure Criterion 5
2.4 Degradation of Properties 6
3 COMPLETE PLY DEGRADATION MODEL 7
3.1 Overview 7
3.2 Model I: Analytical Solution ($D_{16} = D_{26} = 0$ and $B = 0$) 7
3.3 Model II: Rayleigh-Ritz Solution (D_{16}, $D_{26} \neq 0$ and $B \neq 0$) 9
3.4 Degradation Procedure 10
4 PLY REGION DEGRADATION MODEL 11
4.1 Overview 11
4.2 Model I: Rayleigh-Ritz Solution (D_{16}, $D_{26} \neq 0$ and $B = 0$) 12
4.3 Model II: Rayleigh-Ritz solution (D_{16}, $D_{26} \neq 0$ and $B \neq 0$) 12
4.4 Degradation Procedure 13
5 PARAMETRIC STUDY ON SQUARE PLATES 13
5.1 Description 13
5.2 Results Using Complete Ply Degradation Model I 14
5.3 Results Using Complete Ply Degradation Model II 15
5.4 Results Using Ply Region Degradation Model I 16
5.5 Results Using Ply Region Degradation Model II 16
6 DISCUSSION OF RESULTS 19
6.1 Some Comments on Limitations of the Analyses 19
6.2 Observed Failure Sequences 20
6.3 Comparisons of Degradation Models 20
6.4 Comparisons with Misirlis's Results; Use of Ply Region Degradation Model II 22
6.5 Use of Tsai-Wu Failure Criterion 23
7 CONCLUSIONS 23
REFERENCES 24
APPENDIX A: TABULATED RESULTS 26

1 INTRODUCTION

1.1 Background

Plates of fibre-reinforced composite materials are widely used in wind turbine blades and in many other structures including certain types of ships. These structural elements are often subjected to significant in-plane forces. Thus, in the design context, strength analysis that takes account of buckling effects plays a crucial role. For wind turbine blades, the need for this kind of analysis can be expected to increase as offshore installation removes some of the constraints on blade size that transportation considerations have imposed for onshore applications. Such analyses, either for individual structures or for parametric studies, are often conducted using finite element (FE) analysis, but these FE analyses tend to be complex and make heavy demands on both computer resources and the analyst's expertise. There is a need for simplified but reliable analysis methods that can readily be used for parametric studies and for quick estimates of the strength of specific structures.

The elastic buckling strength of fibre reinforced composite plates has been studied extensively in the past and is treated in several textbooks [1,2,3]. Many of these studies have been confined to the determination, by analytical or other means, of elastic critical loads of rectangular plates for simple, in-plane loading cases. These studies, by their nature, neglect the effects of initial geometrical imperfections (out-of-flatness). In analytical studies the laminated plate is generally considered to be composed of a uniform, orthotropic material. Various boundary conditions and in-plane loading cases have been considered.

More recently, attention has turned to the estimation of the ultimate strength of such plates. For this, post-buckling deformation may have to be considered since, for many plates, the carrying capacity can be significantly higher than the elastic critical load. Consideration of such deformation has been extensively studied for metal plates of isotropic material and for stiffened metal plates, which can often be treated as orthotropic by "smearing out" the stiffeners over the plate. The major challenge for composite plates, however, is to deal with the material behaviour: appropriate criteria must be applied to detect initial failure of the material and to describe subsequent degradation of its stiffness properties up to a point at which the maximum load capacity is reached. This generally has to be applied at each ply of the composite layup. For rectangular, unstiffened metal plates loaded in uniaxial compression, simplified treatments of ultimate strength are available based, for example, on the use of an effective width of plating combined with the observation that the maximum in-plane compressive load is reached when the yielding occurs at the middle regions of the edges parallel to the loading direction. For unstiffened and stiffened metal plates, including plates with arbitrary stiffener orientations, a family of simplified ultimate strength limit methods has been developed by Brubak *et al.* [4] and Brubak and Hellesland [5,6,7,8]. For composite plates, however, simplified analyses have, to the authors' knowledge, been confined to linear eigenvalue buckling analysis [9,10].

Detailed studies of the ultimate strength of rectangular composite plates with geometrical imperfections have recently been carried out by a consortium of universities

and research institutes in the EU Network of Excellence on Marine Structures MARSTRUCT. These studies are reported by Hayman *et al*. [11]. They consisted of a series of non-linear FE analyses that were validated against instrumented laboratory tests, followed by a parametric study of simply supported square and rectangular plates using the validated modelling techniques. This parametric study was performed by Misirlis at the University of Newcastle using the Hashin and Rotem 1973 failure criterion [12] and a degradation model applied at ply level in a non-linear finite element (FE) analysis. A subsequent study reported by Misirlis *et al*. [13] explored a series of alternative failure criteria and degradation modelling techniques, including use of the Tsai-Wu failure criterion [14].

1.2 The Present Study

The present paper concerns a part of a study in which simplified methods for the estimation of the ultimate in-plane strength of composite and sandwich plates are being developed. The ultimate goal is to be able to take account of:

- failure and degradation models for composites,
- initial geometric imperfections,
- out-of-plane shear deformations in thick composite and sandwich plates, and
- post-buckling deformations, which are especially important for thin plates.

As mentioned earlier, one of the greatest challenges in dealing with the ultimate strength of composite plates concerns failure and degradation models. In a very simple model an elastic critical load is found but degraded matrix-dominated stiffness properties are assumed for the entire plate. In a slightly more advanced model the degraded material properties are again used, but in an analysis that takes account of the geometrical imperfections, each ply being checked for fibre failure. As a first step towards establishing more accurate simplified methods dealing with the four major effects listed above, the present study is limited to consider simply supported, rectangular plates in uniaxial compression, in which the following simplifications are made:

- Out-of-plane shear deformations and initial out-of-flatness are included but post-buckling deformations are not modelled (i.e. the response is described using small-deflection theory based on linear differential equations).
- While the failure criterion is checked at all locations in each ply, once failure is detected a larger area of the ply is given degraded stiffness properties. Two approaches are used in this respect. In one approach, a *complete ply degradation model* is used, in which the entire ply is given degraded properties. In the second approach, a *ply region degradation model* is used, in which each ply is from the outset divided into a small number of regions and only the affected region of the ply is degraded.
- Failure criteria are limited to in-plane stresses, i.e. possible interlaminar failure is not accounted for. Thus, out-of-plane shear stiffness is not degraded during the analysis.

In addition, the effects of certain simplifications regarding the stiffness matrix are investigated. If the composite layup is symmetric, the bending-stretching coupling matrix (*B*-matrix) is zero. This means that only bending deformations need to be considered. If, in addition to a zero *B*-matrix, the bending-twisting coupling terms (D_{16} and D_{26}) in the bending stiffness matrix are zero, the plate becomes specially orthotropic and an analytic solution is possible. However, although D_{16} and D_{26} are often small for typical layups, they are rarely zero. Furthermore, even if the layup is initially symmetric, the properties become asymmetric and the *B*-matrix non-zero as soon as degradation begins. To investigate the influence of these effects, in combination with the two degradation approaches, four different types of analysis have been performed:

i. *Complete ply degradation model I*: A solution is performed using the complete ply degradation approach, with all terms in the bending-stretching coupling matrix (*B*-matrix) and the bending-twisting coupling terms (D_{16} and D_{26}) in the bending stiffness matrix assumed to be zero. This allows an analytical solution.

ii. *Complete ply degradation model II*: The complete ply degradation approach is used but with $D_{16} \neq 0$, $D_{26} \neq 0$ and $B \neq 0$. An energy solution is performed using assumed deformations in the form of a truncated double Fourier series.

iii. *Ply region degradation model I*: The ply region degradation approach is applied with $B = 0$. An energy solution is performed, so it is possible to retain $D_{16} \neq 0$ and $D_{26} \neq 0$. Deformations are assumed in the form of a truncated double Fourier series.

iv. *Ply region degradation model II*: The same approach is applied as in analysis type (iii) but with $B \neq 0$. Deformations are assumed in the form of a truncated double Fourier series.

For all analysis types the Hashin and Rotem failure criterion [12] is applied, and for analysis type (i) the Tsai-Wu criterion [14] is applied in addition for comparison.

In the parametric study reported in Section 5, square plates of various thicknesses are considered. Two basic types of composite layup are considered:

- A triaxial layup (case A) with about 89% of the reinforcement placed parallel to the loading direction and the remainder divided equally between the +45° and -45° directions. Such layups are typical for wind turbine blades.
- A quasi-isotropic, quadriaxial layup (case B), which is typical for situations in which the direction of loading may vary, or there is a combination of out-of-plane and in-plane loads such as occurs in hull panels of marine craft.

The results are compared with those of Misirlis, reported in [11], from more detailed FE analyses of the same cases. Thus the extent to which the simplified approaches can be used to give reasonable estimates of ultimate strength is established. The analyses also aim to show whether ultimate failure is characterised by particular events in the sequence of ply failures.

2 PROGRESSIVE FAILURE MODELS

2.1 Overall Description

Two different failure criteria are applied in this study. Each is applied at ply level and is connected to a degradation model as described in the following sub-sections.

2.2 Tsai-Wu Failure Criterion

For a two-dimensional stress state, σ_1, σ_2, τ_{12}, where subscript 1 denotes the longitudinal (fibre) direction and 2 the transverse direction, the Tsai-Wu failure criterion can be written [14]:

$$FI = F_{11}\sigma_1^2 + F_{22}\sigma_2^2 + F_{66}\tau_{12}^2 + 2F_{12}\sigma_1\sigma_2 + F_1\sigma_1 + F_2\sigma_2 = 1 \tag{1}$$

where

$$F_{11} = \frac{1}{X_t X_c},\ F_{22} = \frac{1}{Y_t Y_c},\ F_{12} = -\frac{1}{2\sqrt{X_t X_c Y_t Y_c}},\ F_1 = \frac{1}{X_t} - \frac{1}{X_c},\ F_2 = \frac{1}{Y_t} - \frac{1}{Y_c},\ F_{66} = \frac{1}{S_{12}^2}$$

and X_t, X_c are the tensile and compressive strengths in the longitudinal direction, Y_t and Y_c are those in the transverse direction and S_{12} is the in-plane shear strength.

In a progressive failure model, it is desirable to distinguish between failure events in the different directions. For this purpose Eq. (1) can be decomposed into three groups [15]:

$$f_1^{T,C} = F_1\sigma_1 + F_{11}\sigma_1^2 + F_{12}\sigma_1\sigma_2 \tag{2a}$$

$$f_2^{T,C} = F_2\sigma_2 + F_{22}\sigma_2^2 + F_{12}\sigma_1\sigma_2 \tag{2b}$$

$$f_6 = F_{66}\tau_{12}^2 \tag{2c}$$

When the failure index defined in Eq. (1) exceeds unity, the largest value of the individual components in Eqs. (2) indicates the dominant failure mode. Material properties in that direction are then degraded.

2.3 Hashin and Rotem Failure Criterion

The 1973 Hashin and Rotem failure criterion for in-plane stresses can be written [12]:

$$f_1^T = \left(\frac{\sigma_1}{X_t}\right)^2 = 1 \tag{3a}$$

$$f_1^C = \left(\frac{\sigma_1}{X_c}\right)^2 = 1 \tag{3b}$$

$$f_2^T = \left(\frac{\sigma_2}{Y_t}\right)^2 + \left(\frac{\tau_{12}}{S_{12}}\right)^2 = 1 \tag{3c}$$

$$f_2^C = \left(\frac{\sigma_2}{Y_c}\right)^2 + \left(\frac{\tau_{12}}{S_{12}}\right)^2 = 1 \tag{3d}$$

Failure occurs when any of the four failure functions from Eqs. (3) reaches unity. Each is associated with a dominant failure mode.

2.4 Degradation of Properties

When failure occurs in a laminated composite plate, the effective material properties change. This results in a new stiffness of the plate. To describe this behaviour, a damaged material stiffness matrix for in-plane deformations is defined [11]:

$$[R] = \begin{bmatrix} (1-d_1)R_{11} & (1-d_1)(1-d_2)R_{12} & 0 \\ sym. & (1-d_2)R_{22} & 0 \\ sym. & sym. & (1-d_6)R_{66} \end{bmatrix} \tag{4}$$

Here d_1 is the damage factor in the longitudinal direction of the material, d_2 is the damage factor in the transverse direction, and d_6 is the damage factor in the in-plane shear component. The remaining parameters in Eq. (4) are defined as $R_{11} = \frac{E_1}{\Delta}$, $R_{22} = \frac{E_2}{\Delta}$, $R_{12} = \frac{\nu_{12}E_2}{\Delta}$, $R_{66} = G_{12}$, and $\Delta = 1 - \nu_{12}\nu_{21}(1-d_1)(1-d_2)$.

For the Hashin criterion, because the shear failure component is associated with the fibre and matrix modes of failure, the damage variable d_6 is defined as:

$$d_6 = 1 - (1-d_1)(1-d_2) \tag{5}$$

The transverse (out-of-plane) shear stiffness matrix is defined in Eq. (6), and following Misirlis [11], this is not degraded during the analysis. (The ABAQUS shell elements used by Misirlis do not allow such degradation of the transverse shear properties.)

$$[K] = \begin{bmatrix} K_{44} & 0 \\ 0 & K_{55} \end{bmatrix} \tag{6}$$

where $K_{44} = G_{23}$ and $K_{55} = G_{13}$.

The instantaneous degradation of material properties is used in the progressive failure model reported here. When any ply or region fulfils a stress criterion, its

corresponding properties are instantaneously reduced to a predefined value equal to 1 % of the respective initial values [16]. Thus the associated damage factor $d_i = 0.99$. In contrast, the FEA results presented in [11] used the built in progressive failure model in ABAQUS with a linear degradation of the material properties [17].

3 COMPLETE PLY DEGRADATION MODEL

3.1 Overview

The models presented in the following sub-sections are based on either solving the buckling differential equations expressed for a specially orthotropic laminate or using the Rayleigh-Ritz method. In the ply which has exceeded a given stress criterion, the degradation of the corresponding properties is then applied to the entire ply. The load is then applied with the reduced stiffness until either a further criterion is exceeded in the same ply or failure occurs in a different ply. Again, the associated material degradation is applied to the entire ply. The process is repeated until the maximum value of load is reached; this is considered to be the ultimate load.

3.2 Model I: Analytical Solution ($D_{16} = D_{26} = 0$ and $B = 0$)

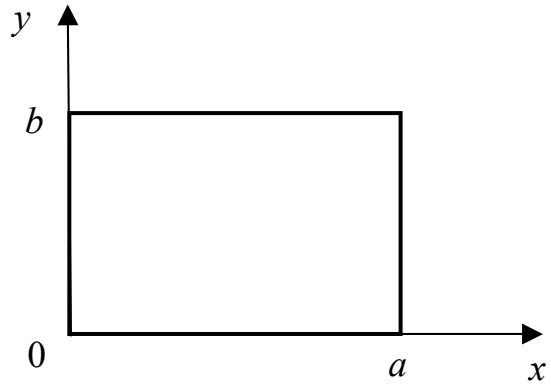

Fig. 1. Plate geometry.

A simply supported plate is considered, with dimensions $a \times b$ (Fig. 1) and an initial out-of-plane deformation w_{init}. When the plate is subjected to an in-plane compressive load N in the x-direction, it experiences an additional deformation w. Thus, the total out-of-plane deformation is $w_{tot}=w_{init}+w$. The following equations are solved for the out-of-plane displacements:

$$D_{11}\frac{\partial^2\phi_x}{\partial x^2}+\left(D_{12}+D_{66}\right)\frac{\partial^2\phi_y}{\partial x\partial y}+D_{66}\frac{\partial^2\phi_x}{\partial y^2}-A_{55}k\left(\phi_x+\frac{\partial w}{\partial x}\right)=0 \tag{7a}$$

$$D_{22}\frac{\partial^2\phi_y}{\partial y^2}+\left(D_{12}+D_{66}\right)\frac{\partial^2\phi_x}{\partial x\partial y}+D_{66}\frac{\partial^2\phi_y}{\partial x^2}-A_{44}k\left(\phi_y+\frac{\partial w}{\partial y}\right)=0 \tag{7b}$$

$$A_{55}k\left(\frac{\partial\phi_x}{\partial x}+\frac{\partial^2 w}{\partial x^2}\right)+A_{44}k\left(\frac{\partial\phi_y}{\partial y}+\frac{\partial^2 w}{\partial y^2}\right)-N\frac{\partial^2 w_{tot}}{\partial x^2}=0 \tag{7c}$$

where D_{ij} is the bending stiffness matrix, A_{ij} ($i = j = 4, 5$) is the stiffness matrix for transverse shear, k is the shear correction coefficient, assumed equal to 5/6, and ϕ_x and ϕ_y are the rotations of a transverse normal about axes parallel to the y and x axes, respectively. It is assumed that the layup is symmetric so that the bending-stretching coupling coefficients B_{ij} are all zero. It is further assumed that the bending-twisting coupling coefficients can be ignored, $D_{16} = D_{26} = 0$.

For a simply supported plate, the following double Fourier series are assumed to represent ϕ_x, ϕ_y and w_{tot} [1]:

$$\phi_x(x,y)=\sum_{n=1}^{\infty}\sum_{m=1}^{\infty}x_{mn}\cos\left(\frac{m\pi x}{a}\right)\sin\left(\frac{n\pi y}{b}\right) \tag{8a}$$

$$\phi_y(x,y)=\sum_{n=1}^{\infty}\sum_{m=1}^{\infty}y_{mn}\sin\left(\frac{m\pi x}{a}\right)\cos\left(\frac{n\pi y}{b}\right) \tag{8b}$$

$$\begin{aligned} w_{tot}(x,y) &= w(x,y)+w_{init}(x,y) \\ &= \sum_{n=1}^{\infty}\sum_{m=1}^{\infty}w_{mn}\sin\left(\frac{m\pi x}{a}\right)\sin\left(\frac{n\pi y}{b}\right)+\sum_{n=1}^{\infty}\sum_{m=1}^{\infty}w_{imn}\sin\left(\frac{m\pi x}{a}\right)\sin\left(\frac{n\pi y}{b}\right) \end{aligned} \tag{8c}$$

where x_{mn}, y_{mn} and w_{mn} are unknown coefficients, m and n are positive integers, and w_{imn} are given imperfection amplitudes.

Substituting these expressions for ϕ_x, ϕ_y and w_{tot} into Eqs. (7a)-(7c) gives the following matrix equation:

$$\begin{bmatrix} C_1 & C_2 & C_3 \\ C_2 & C_4 & C_5 \\ C_3 & C_5 & N\alpha^2+\alpha C_3+\beta C_5 \end{bmatrix}\begin{Bmatrix} x_{mn} \\ y_{mn} \\ w_{mn} \end{Bmatrix}=\begin{Bmatrix} 0 \\ 0 \\ -N\alpha^2 w_{imn} \end{Bmatrix} \tag{9}$$

where $\alpha=\dfrac{m\pi}{a}$, $\beta=\dfrac{n\pi}{b}$, $C_1=-D_{11}\alpha^2-D_{66}\beta^2-A_{55}k$, $C_2=-D_{12}\alpha\beta-D_{66}\alpha\beta$, $C_3=-A_{55}k\alpha$, $C_4=-D_{22}\beta^2-D_{66}\alpha^2-A_{44}k$ and $C_5=-A_{44}k\beta$.

The coefficients x_{mn}, y_{mn} and w_{mn} can be solved for a given applied load N and set of initial imperfection amplitudes w_{imn}, thus giving the corresponding double Fourier series for a simply supported plate with given geometric imperfection. If the initial imperfection is described by a single term, i.e. a single pair of values of m and n, the solution involves only the corresponding terms.

3.3 Model II: Rayleigh-Ritz Solution (D_{16}, $D_{26} \neq 0$ and $B \neq 0$)

Rayleigh-Ritz method has been chosen to solve the problem, since the D_{16} and D_{26} terms and the bending-stretching coupling coefficients B_{ij} are included in the analysis. For a simply supported plate with a geometric imperfection subjected to uniaxial compressive load, the boundary conditions are still satisfied with the same corresponding double Fourier series presented in Eqs. (8a)-(8c) in addition to the following [8]:

$$u_0(x,y) = \sum_{n=1}^{\infty}\sum_{m=1}^{\infty} u_{mn} \sin\left(\frac{m\pi x}{a}\right)\sin\left(\frac{n\pi y}{b}\right) + u_c \frac{x}{a} \tag{10a}$$

$$v_0(x,y) = \sum_{n=1}^{\infty}\sum_{m=1}^{\infty} v_{mn} \sin\left(\frac{m\pi x}{a}\right)\sin\left(\frac{n\pi y}{b}\right) + v_c \frac{y}{b} \tag{10b}$$

The mid-plane displacements in the x- and y-direction is now represented by u_0 and v_0, where u_{mn}, v_{mn}, u_c and v_c are unknown coefficients.

The total potential energy consists of three contributions associated, respectively, with in-plane strain energy, shear strain energy and external forces:

$$\Pi = U_b + U_s + U_p \tag{11}$$

where

$$\begin{aligned} U_b &= \frac{1}{2}\int_V \varepsilon_b^T \sigma_b \, dV = \frac{1}{2}\int_A \int_{-h/2}^{h/2} \varepsilon_b^T \overline{Q} \varepsilon_b \, dz \, dA \\ &= \frac{1}{2}\int_A \left[\varepsilon_0^T A \varepsilon_0 + 2\varepsilon_0^T B \kappa + \kappa^T D \kappa \right] dA \\ &= U_{b,1} + U_{b,2} + U_{b,3} \end{aligned} \tag{12}$$

$$\begin{aligned} U_{b,1} = \frac{1}{2}\int \varepsilon_0^T A \varepsilon_0 \, dA = \frac{1}{2}\int_0^b \int_0^a \Bigg[& A_{11}\left(\frac{\partial u_0}{\partial x}\right)^2 + 2A_{12}\left(\frac{\partial u_0}{\partial x}\right)\left(\frac{\partial v_0}{\partial y}\right) + A_{22}\left(\frac{\partial v_0}{\partial y}\right)^2 \\ & + 2A_{16}\frac{\partial u_0}{\partial x}\left(\frac{\partial u_0}{\partial y} + \frac{\partial v_0}{\partial x}\right) + 2A_{26}\frac{\partial v_0}{\partial y}\left(\frac{\partial u_0}{\partial y} + \frac{\partial v_0}{\partial x}\right) + A_{66}\left(\frac{\partial u_0}{\partial y} + \frac{\partial v_0}{\partial x}\right)^2 \Bigg] dx dy \end{aligned} \tag{13a}$$

$$U_{b,2} = \frac{1}{2}\int 2\varepsilon_0^T B\kappa\, dA = \int_0^b\int_0^a \Bigg[B_{11}\frac{\partial u_0}{\partial x}\frac{\partial \phi_x}{\partial x} + B_{12}\left(\frac{\partial v_0}{\partial y}\right)\left(\frac{\partial \phi_x}{\partial x}\right) + B_{12}\left(\frac{\partial u_0}{\partial x}\right)\left(\frac{\partial \phi_y}{\partial y}\right)$$
$$+ B_{22}\left(\frac{\partial v_0}{\partial y}\right)\left(\frac{\partial \phi_y}{\partial y}\right) + B_{16}\frac{\partial \phi_x}{\partial x}\left(\frac{\partial u_0}{\partial y} + \frac{\partial v_0}{\partial x}\right) + B_{16}\frac{\partial u_0}{\partial x}\left(\frac{\partial \phi_x}{\partial y} + \frac{\partial \phi_y}{\partial x}\right)$$
$$+ B_{26}\frac{\partial \phi_y}{\partial y}\left(\frac{\partial u_0}{\partial y} + \frac{\partial v_0}{\partial x}\right) + B_{26}\frac{\partial v_0}{\partial y}\left(\frac{\partial \phi_x}{\partial y} + \frac{\partial \phi_y}{\partial x}\right)$$
$$+ B_{66}\left(\frac{\partial u_0}{\partial y} + \frac{\partial v_0}{\partial x}\right)\left(\frac{\partial \phi_x}{\partial y} + \frac{\partial \phi_y}{\partial x}\right)\Bigg] dxdy \tag{13b}$$

$$U_{b,3} = \frac{1}{2}\int_A \kappa^T D\kappa\, dA = \frac{1}{2}\int_0^b\int_0^a \Bigg[D_{11}\left(\frac{\partial \phi_x}{\partial x}\right)^2 + 2D_{12}\left(\frac{\partial \phi_x}{\partial x}\right)\left(\frac{\partial \phi_y}{\partial y}\right) + D_{22}\left(\frac{\partial \phi_y}{\partial y}\right)^2$$
$$+ 2D_{16}\frac{\partial \phi_x}{\partial x}\left(\frac{\partial \phi_x}{\partial y} + \frac{\partial \phi_y}{\partial x}\right) + 2D_{26}\frac{\partial \phi_y}{\partial y}\left(\frac{\partial \phi_x}{\partial y} + \frac{\partial \phi_y}{\partial x}\right) \tag{13c}$$
$$+ D_{66}\left(\frac{\partial \phi_x}{\partial y} + \frac{\partial \phi_y}{\partial x}\right)^2\Bigg] dxdy$$

$$U_s = \frac{1}{2}\int_V \varepsilon_s^T \sigma_s\, dV = \frac{1}{2}\int_A\int_{-h/2}^{h/2} \varepsilon_s^T \overline{Q}_s \varepsilon_s\, dz\, dA = \frac{1}{2}\int_A \varepsilon_s^T A_s \varepsilon_s\, dA$$
$$= \frac{1}{2}k\int_0^b\int_0^a \left[A_{44}\left(\phi_y + \frac{\partial w}{\partial y}\right)^2 + A_{55}\left(\phi_x + \frac{\partial w}{\partial x}\right)^2\right] dxdy \tag{14}$$

$$U_p = -\frac{1}{2}\int_0^b\int_0^a N\left(\frac{\partial w_{tot}}{\partial x}\right)^2 dx\, dy + \int_0^b\int_0^a N\left(\frac{\partial u_0}{\partial x}\right) dx\, dy \tag{15}$$

Equilibrium requires that $\delta\Pi = 0$, thus

$$\frac{\partial \Pi}{\partial u_c} = \frac{\partial \Pi}{\partial v_c} = 0 \tag{16a}$$

$$\frac{\partial \Pi}{\partial u_{mn}} = \frac{\partial \Pi}{\partial v_{mn}} = \frac{\partial \Pi}{\partial x_{mn}} = \frac{\partial \Pi}{\partial y_{mn}} = \frac{\partial \Pi}{\partial w_{mn}} = 0, \quad m = 1,...,\infty\ ,\ n = 1,...,\infty \tag{16b}$$

The coefficients u_c, v_c, u_{mn}, v_{mn}, x_{mn}, y_{mn} and w_{mn} can be found by solving Eqs. (16).

3.4 Degradation Procedure

For the models with complete ply degradation, the degradation procedure is presented in the schematic diagram (Fig. 2). The process shown is repeated until no further increase in N is possible. This determines the ultimate load.

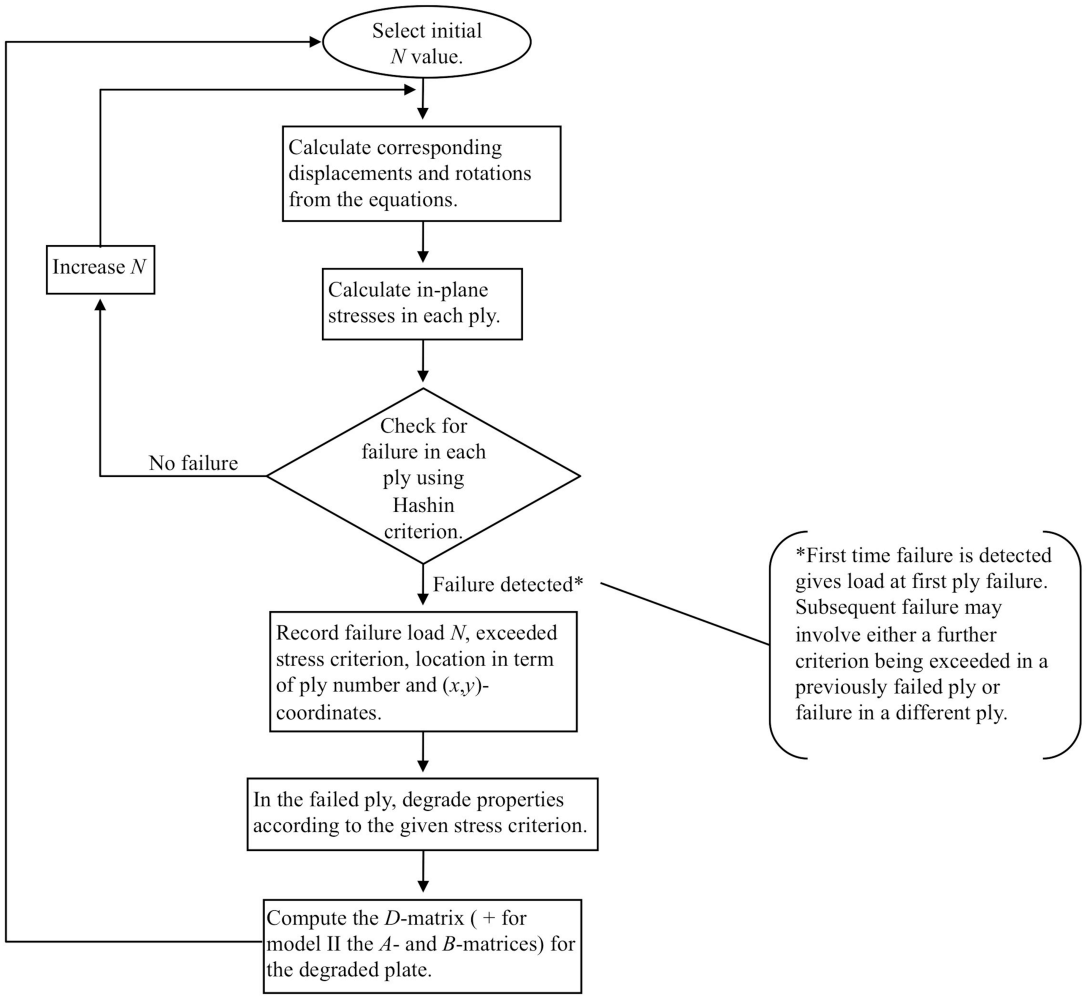

Fig. 2. Schematic diagram: degradation procedure for complete ply degradation model.

4 PLY REGION DEGRADATION MODEL

4.1 Overview

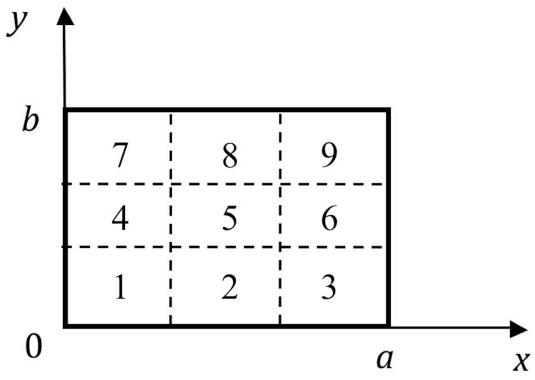

Fig. 3. Plate geometry for ply region degradation model.

The models presented in the following sub-sections are based on Fig. 3. A plate with

dimensions $a \times b$ has been divided into 9 regions. The degradation is now limited to specific regions. Rather than solving the differential equations as in Section 3.2, it is now more convenient to use the Rayleigh-Ritz method since after first ply failure the material properties are not constant over the entire area of the plate. For increasing applied load, each ply is checked for failure. In the region of a ply in which a given strength criterion has been exceeded, the corresponding properties in that region of that ply are degraded. At the next load step, either a further criterion is exceeded in the same region or failure occurs in a different ply and/or region; here the associated properties are also instantaneously degraded. The process is continued until the occurrence of ultimate (maximum) load.

4.2 Model I: Rayleigh-Ritz Solution (D_{16}, $D_{26} \neq 0$ and $B = 0$)

The Rayleigh-Ritz method has been chosen to solve the problem, since the progressive failure model is based on ply region degradation. For simply supported plates with a geometric imperfection subjected to uniaxial compressive load, the boundary conditions are satisfied with the same corresponding double Fourier series presented in Eqs. (8a)-(8c). The total potential energy is again given by Eqs. (11)-(15), where $U_{b,1}$ and $U_{b,2}$ are now zero, and the last term in Eq. (15), associated with the x-direction displacement field, can be neglected since the in-plane displacement field is not included in the present model.

Equilibrium requires that $\delta\Pi = 0$, which reduces to

$$\frac{\partial \Pi}{\partial x_{mn}} = \frac{\partial \Pi}{\partial y_{mn}} = \frac{\partial \Pi}{\partial w_{mn}} = 0, \quad m = 1,...,\infty \ , \ n = 1,...,\infty \tag{17}$$

The coefficients x_{mn}, y_{mn} and w_{mn} can be found by solving Eq. (17). The progressive failure model with degraded material properties is now implemented by removing the appropriate terms in the Eqs. (13c), (14) and (15) in the specific region of the ply where failure has occurred.

4.3 Model II: Rayleigh-Ritz solution (D_{16}, $D_{26} \neq 0$ and $B \neq 0$)

For a simply supported plate with a geometric imperfection subjected to uniaxial compressive load, the kinematic boundary conditions are satisfied with the double Fourier series given in Eqs. (8a)-(8c) and (10a)-(10b). The total potential energy is again given by Eq. (11), where U_b is given by Eqs. (13a)-(13c), and U_s, U_p are given by Eqs. (14)-(15).

Equilibrium requires that $\delta\Pi = 0$, thus the unknown coefficients u_c, v_c, u_{mn}, v_{mn}, x_{mn}, y_{mn} and w_{mn} can be found by solving Eqs. (16). The progressive failure model with degraded material properties is now implemented by removing the appropriate terms in the Eqs. (13)-(15) in the specific region of the ply where failure has occurred, rather than for the entire ply as with the complete ply degradation model in Section 3.3.

4.4 Degradation Procedure

The degradation procedure is similar to that described in Section 3.4, but degradation at each stage is applied only over that region of a ply that has fulfilled the failure criterion, as indicated in Sections 4.2 and 4.3.

5 PARAMETRIC STUDY ON SQUARE PLATES

5.1 Description

The parametric studies are performed, using Matlab, for a series of square plates, with $a = b = 500$ mm, having various breadth/thickness (b/t) ratios. The plates are simply supported on all edges and subjected to uniform compression N in the x-direction. In the analyses using complete ply degradation model II and ply region degradation model II, this is achieved by restraining the edge $x = 0$ in the x-direction and applying a uniform compressive loading N in the x-direction on the edge $x = a$, all edges being held straight. The cases considered are identical to some of those considered by Misirlis in [11].

Two different types of layup have been investigated:

- Case A, triaxial layup: $\left[-45 / +45 / 0_4 / +45 / -45 / 0_4 / -45 / +45 / 0_3\right]_S$
- Case B, quasi-isotropic, quadriaxial layup: $\left[0 / +45 / 90 / -45\right]_{X,S}$

For the triaxial layups (case A), the required b/t values are achieved by scaling the thickness of each individual ply. Further, to reduce calculation time, each group of 0° plies between the ±45° plies has been combined into a single ply. The total number of plies considered in the analysis is now 18 instead of 34 for these layups. This combination has only been applied for the complete ply degradation model I and II and the ply region degradation model I. For the quadriaxial layups (case B), the thickness is instead increased by adding groups of plies (increasing X) to give the desired b/t values. The material properties and the plate thicknesses for cases A and B are given in Tables 1-3. Note that ply number 1 is located on the concave side of the plate.

Table 1
Material properties (strengths and moduli).

Property	E_1	E_2	ν_{12}	G_{12}	G_{13}	G_{23}	X_t	X_c	Y_t	Y_c	S_{12}
Value	49627	15430	0.272	4800	4800	4800	968	915	24	118	65
Units	MPa	MPa	-	MPa	MPa	MPa	MPa	MPa	MPa	MPa	MPa

Table 2
Plate thicknesses and ply thicknesses for case A.

b/t	t (mm)	t_0 (mm)	$t_{\pm 45}$ (mm)
10	49.98	1.95	0.59
15	33.40	1.30	0.40
20	24.94	0.97	0.30
30	16.70	0.65	0.20
50	10.02	0.39	0.12

Table 3
Plate thicknesses and ply thicknesses for case B.

b/t	t (mm)	X	t_0, $t_{\pm 45}$, t_{90} (mm)
62.50	8.00	1	1.00
31.25	16.00	2	1.00
20.83	24.00	3	1.00
15.63	32.00	4	1.00
10.42	48.00	6	1.00

The assumed shape of the initial geometric imperfection is a single half sine wave in each direction, so that $w_{imn} = 0$ for all values of m and n other than 1. Four different maximum initial imperfection amplitudes have been examined. They are respectively 0.1%, 1%, 2% and 3% of the width b (= 500 mm).

For the complete ply degradation model I the analytical solution is adopted, and the solution is relatively straightforward because only the terms corresponding to $m = n = 1$ are non-zero in the double Fourier series for the deformations. For the ply region degradation model I the Rayleigh-Ritz solution is used, with the coupling terms D_{16} and D_{26} included. This results in the possibility of more non-zero terms in the double Fourier series of the deformations. However, only a single term has been retained in the solution in this model. For the complete ply degradation model II and the ply region degradation model II, however, 49 terms have been included in each double Fourier series. Thus, the total number of unknown coefficients is 247.

For both ply region degradation models (I and II), the size of regions 1, 3, 7 and 9 is 160 mm × 160 mm. Regions 2 and 8 are each 180 mm × 160 mm, while regions 4 and 6 are each 160 mm × 180 mm. Finally, region 5 has the size 180 mm × 180 mm.

5.2 Results Using Complete Ply Degradation Model I

The results from the complete ply degradation model I combined with the Hashin criterion and the Tsai-Wu criterion are given in full in Appendix A.

Table A.1 gives the results for the case A layups, using the complete ply degradation model I combined with the Hashin criterion. Table A.2 shows the corresponding results for the case B layups. For the Tsai-Wu criterion, the results are given in Table A.3 for case A, and in Table A.4 for case B layups. For a given initial geometric imperfection amplitude, plate thickness (t) and total number of plies, the following are shown in these tables:

- At first ply failure (FPF), the calculated stress (σ_{FPF}) and location of first failure in terms of ply number and direction of that ply.
- The ultimate stress (σ_{max}) estimated by investigating a last ply failure condition ("LPF"). Also shown are the ply in which this last ply failure occurs (as ply number and direction) and the number of plies that have failed at this stage.

Further, in Tables A.1 and A.2, the results from the analysis are compared with those conducted by Misirlis (σ_{max} from [11]). The ratio of the ultimate strength from the

present model to that found by Misirlis is given in the last column (σ_{max} /σ_{max} from [11]). These are again shown in Figs. 4-5 for various values of the plate thickness t and imperfection amplitude. For cases using the Tsai-Wu criterion, i.e. Tables A.3 and A.4, the results are compared to those from Tables A.1 and A.2 using the complete ply degradation model I with the Hashin criterion.

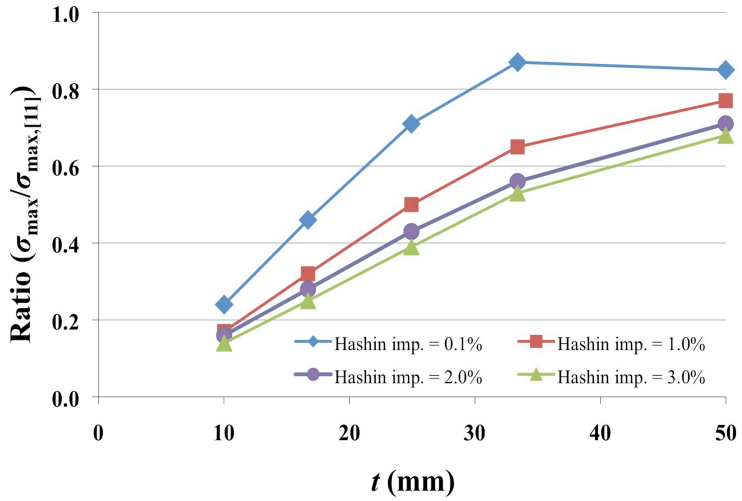

Fig. 4. Case A (triaxial layups), Hashin criterion combined with the complete ply degradation model I. The ultimate strengths from the present analyses are compared to those of Misirlis [11] for a range of plate thicknesses t and imperfection amplitudes.

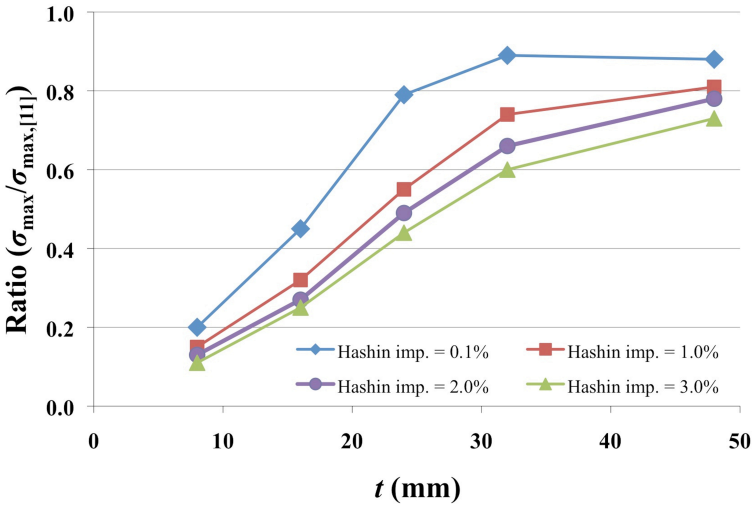

Fig. 5. Case B (quadriaxial layups), Hashin criterion combined with the complete ply degradation model I. The ultimate strengths from the present analyses are compared to those of Misirlis [11] for a range of plate thicknesses t and imperfection amplitudes.

5.3 Results Using Complete Ply Degradation Model II

A summary of the results from the complete ply degradation model II combined with the Hashin criterion is given in Tables A.5 and A.6 in Appendix A for cases A and B, respectively. The ultimate stresses are compared with those achieved in Tables A.1 and

A.2 using the complete ply degradation model I. Only a limited number of cases have been investigated.

5.4 Results Using Ply Region Degradation Model I

Tables A.7 and A.8 in Appendix A show the results for cases A and B, respectively, using the ply region degradation model I combined with the Hashin criterion. The last column provides the deviations compared to those from Tables A.1 and A.2 using the complete ply degradation model I. Only a few cases have been applied for investigation.

5.5 Results Using Ply Region Degradation Model II

Tables A.9 and A.10 in Appendix A give the results for cases A and B, respectively, using the ply region degradation model II combined with the Hashin criterion. For a given initial geometric imperfection amplitude, some changes have been made from the previous tables. In addition to the number of plies, these tables also provide the total number of ply regions for each plate thickness. For the ultimate stress (σ_{max}), it is interesting to show the number of matrix failed ply regions and fibre failed ply regions. Further, the results from the analysis are compared with those conducted by Misirlis (σ_{max} from [11]). The ratio of the ultimate strength from the present model to that found by Misirlis is given in the last column (σ_{max} /σ_{max} from [11]). These are again shown in Figs. 6-7 for various values of the plate thickness t and imperfection amplitude.

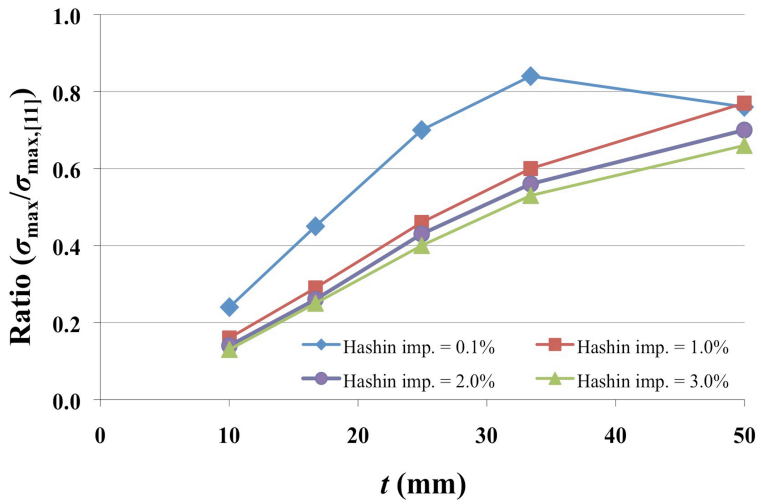

Fig. 6. Case A (triaxial layups), Hashin criterion combined with the ply region degradation model II. The ultimate strengths from the present analyses are compared to those of Misirlis for various plate thicknesses t and imperfection amplitudes.

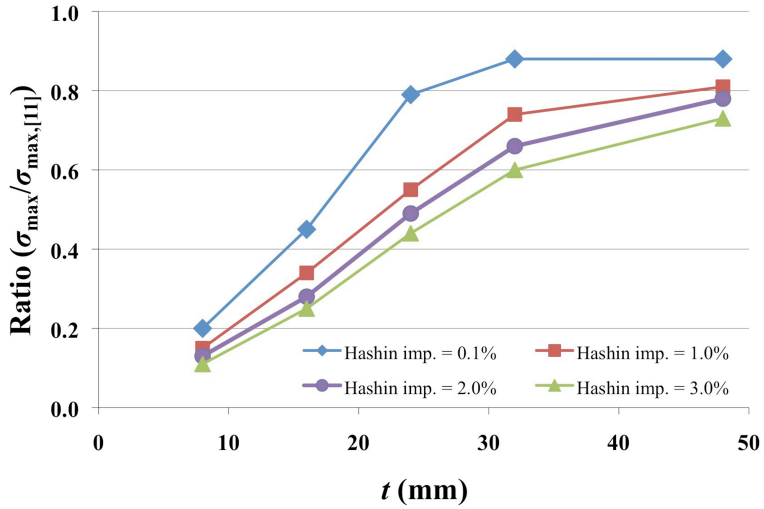

Fig. 7. Case B (quadriaxial layups), Hashin criterion combined with the ply region degradation model II. The ultimate strengths from the present analyses are compared to those of Misirlis for a range of plate thicknesses t and imperfection amplitudes.

In Figs. 8-9, the applied load is plotted against the end shortening and displacement in the centre for some selected cases. Further, in Figs. 10-11, the ultimate strengths for a predefined range of b/t are presented. Figure 10 is based on Table A.9 and Fig. 11 is based on Table A.10.

More investigations have been performed to see the real effects of B-matrix and D_{16} and D_{26} related to the ply region degradation model II (either $B = 0$ or $D_{16} = D_{26} = 0$). The results are presented in Tables A.11 and A.12 in Appendix A. They are compared with the corresponding results from Tables A.9 and A.10.

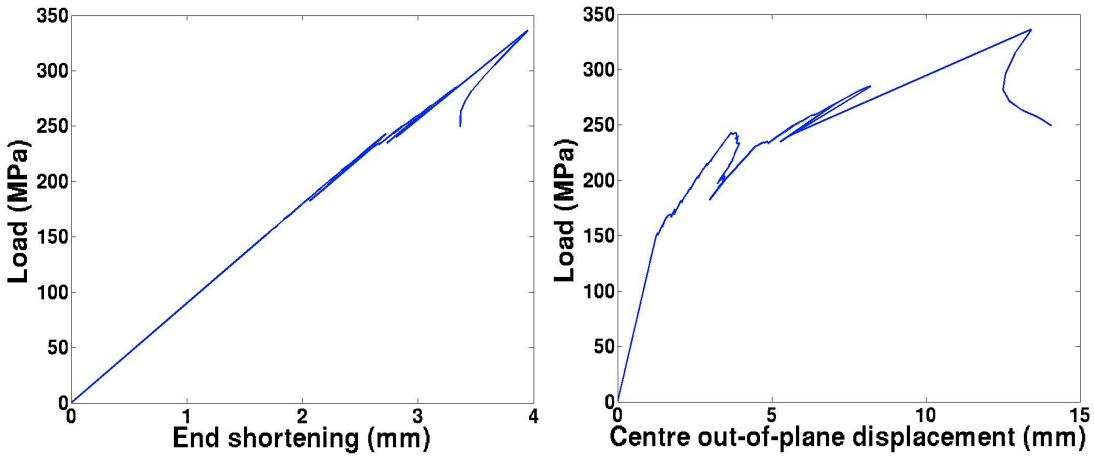

Fig. 8. Load vs. end shortening (left) and load vs. centre out-of-plane displacement (right) for case A (triaxial layups) with $t = 49.98$ mm and 1% imperfection amplitude using Hashin criterion and ply region degradation model II.

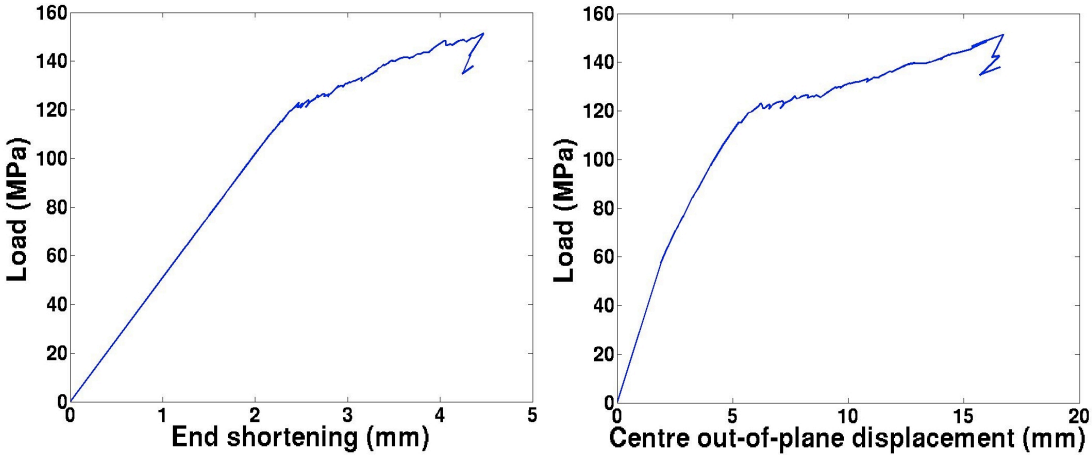

Fig. 9. Load vs. end shortening (left) and load vs. centre out-of-plane displacement (right) for case B (quadriaxial layups) with t = 32 mm and 2% imperfection amplitude using Hashin criterion and ply region degradation model II.

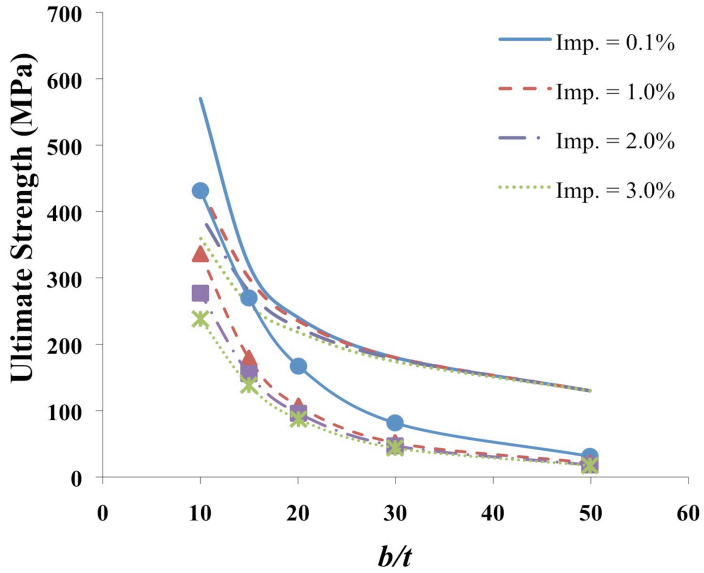

Fig. 10. Case A (triaxial layups) with Hashin criterion and the ply region degradation model II. Graphs without markers are from Misirlis.

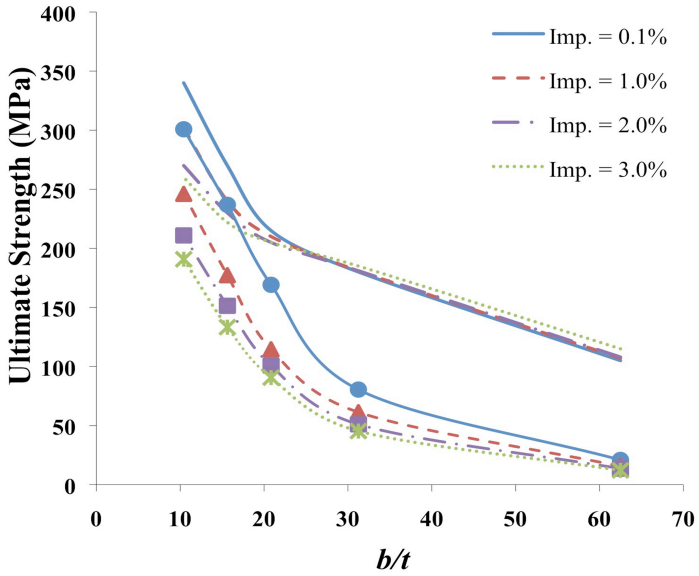

Fig. 11. Case B (quadriaxial layups) with Hashin criterion and the ply region degradation model II. Graphs without markers are from Misirlis.

6 DISCUSSION OF RESULTS

6.1 Some Comments on Limitations of the Analyses

In the complete ply degradation model I and the ply region degradation model I, it has been assumed that the bending-stretching coupling coefficients B_{ij} are all zero. As all the layups are symmetric, this assumption is initially correct, but as individual plies become degraded the symmetry is lost and the solution becomes less accurate. To avoid this limitation the B-matrix is included in the other models.

In the complete ply degradation model I, the terms D_{16} and D_{26} (which are not inherently zero for the layups considered) have been neglected. In the initial layups these terms are believed to be small, but the situation may change as ply degradation proceeds. Some investigation of this is made with the complete ply degradation model II and both of the ply region degradation models, which are based on the Rayleigh-Ritz method. However, to have a significant effect of D_{16} and D_{26} it is necessary to include more than one term in the corresponding double Fourier series [18]. This implies that in the ply region degradation model I, the effects of D_{16} and D_{26} have not been accounted for, even though the terms have been included.

There is a difference between the boundary conditions assumed here (the complete ply degradation model I and the ply region degradation model I) and in the analyses by Misirlis [11]. In the present analysis a uniform compressive force per unit length N is applied at the edges $x = 0$ and $x = 500$, while the edges $y = 0$ and $y = 500$ are stress-free. In contrast, Misirlis's FE analysis performed in ABAQUS assumes that all four edges are kept straight, though they are allowed to move in the plane of the plate. However, since both degradation models used in the present analyses neglect the post-buckling behaviour, this difference between in-plane constraints does not influence the predicted behaviour.

For case A, combining zero plies in the analyses using complete ply degradation model I and II and the ply region degradation model I, will cause some inaccuracies. However the effect is believed to be small since the material properties and the geometry are unchanged. Note that in the ply region degradation model II analyses for case A, the combined zero plies are split up so the total number of plies is increased from 18 to 34.

6.2 Observed Failure Sequences

For thin plates with case A (triaxial) layups, according to the tables in Appendix A, one of the outermost 45° plies always fails first, while a 0° ply fails first for the thicker plates. According to Table A.9 in Appendix A, when the 0° plies are not combined, almost all case A layups have a 0° ply as their first ply failure. Failure usually occurs in the outer plies, primarily in the top plies (the convex side of the plate). The 0° plies often fail first in the centre of the plate, while ±45° plies fail in the corners. Further, for thin plates with small imperfections, there is little or no reserve strength beyond the first ply failure condition. In contrast, to achieve the ultimate strength of the thick plates and the plates with large imperfections, all or almost all plies/ply regions have to fail (matrix failure). The ultimate strength is usually attained at the incidence of fibre failure.

For the case B (quadriaxial) layups, for which results are presented in Appendix A, plates with all thicknesses and imperfections fail first in 0° plies except for two cases. The exceptions are the two thickest plates with the smallest imperfection, which fail first in a 90° ply. As for the case A layups, failure usually occurs in the outer plies, most of all top plies (the convex side of the plate). The 0° and 90° plies often fail first in the centre of the plate, while the ±45° plies fail in the corners. For thin plates with a small imperfection, there is almost no reserve of strength beyond the first ply failure stresses. Also the number of plies or ply regions that must have matrix failure before the plate reaches its ultimate load increases with the plate thickness. For plates with large imperfections, and all thicknesses except the thinnest ones, many plies have to fail (matrix failure) before the plate reaches its ultimate strength. According to Table A.10, for thick plates, in addition to many matrix failed ply regions, the ultimate strength is achieved when fibre failure occurs in a ply region.

6.3 Comparisons of Degradation Models

All analyses considered in this discussion use the Hashin failure criterion. Note that some comparisons are based on very few calculated cases. Estimation of the ultimate stress (σ_{max}) is made by investigating a last ply failure condition as described in the earlier sections.

Both complete ply region models as well as the ply region degradation model I served as test models. It is interesting to see the effects of the B-matrix, the terms D_{16} and D_{26}, and material degradation applied to a region in a ply compared to degradation of the entire ply.

For case A - first ply failure:

- There is no detectable difference between the complete ply degradation models I and II and the ply region degradation model I.
- The ply region degradation model II gives 0% - 10% lower values of first ply failure load. The difference may be due to the fact that the combined zero plies are split up in the latter model, and then the appearance of first ply failure may vary.
- Setting $B = 0$ and/or $D_{16} = D_{26} = 0$ in the ply region degradation model II makes no difference (see Table A.11 in Appendix A). This may be explained by the fact that only the first term in the series is activated up to first ply failure. It is only when the material properties vary over the panel that higher modes of deformation are activated.

For case A - "last ply failure":

- The complete ply degradation model II gives 0% - 11% lower ultimate loads than complete ply degradation model I. This means that including the B-matrix and D_{16} and D_{26} causes lower predicted plate strength. However, no clear trends are seen regarding the size of the reduction.
- As discussed in Section 6.4 below, the ultimate loads predicted by the current analyses lie below those found by Misirlis [11]. The ply region degradation model I has been investigated for a limited number of cases to establish whether this slightly more detailed description of the degradation can give a higher prediction of the ultimate load. However, the improvement achieved is either negligible or quite small. Compared to the complete ply degradation model I, the predicted ultimate stresses are the same for the thin plates with small geometric imperfections because the maximum load is reached at or shortly after first ply failure. For thin plates with a larger imperfection, the ply region degradation does give improved results, but the greatest increase in predicted ultimate load is still only about 1.4%. Because of the larger imperfections, the number of failed plies increases and confining the material degradation to a limited region in a ply does predict a larger value of ultimate strength. For the thickest plates, there is no difference between the results given by the two degradation models, even for a larger imperfection. This could be explained by the fact that the imperfections are small compared to the plate thickness so that the stress distribution over the area of the plate, within a given ply, is close to uniform, with the result that the ply region model will predict failure in all regions of a given ply within a small range of applied loads.
- The ply region degradation model II gives generally lower values than the ply region degradation model I, the difference being in the range 0% - 11%. This is due to the effects of the B-matrix and D_{16} and D_{26}.
- Setting $D_{16} = D_{26} = 0$ in the ply region degradation model II has little effect, while setting $B = 0$ increases values for a 1% imperfection, but gives virtually unchanged values for a 3% imperfection.

For case B - first ply failure:

- There is no detectable difference between the first ply failure loads given by the four models.

For case B - “last ply failure”:

- The complete ply degradation model II gives generally very slightly (0% - 2%) lower ultimate loads than the complete ply degradation model I. However, for the largest (3%) imperfection with the thinnest plate, the reduction is 6.5%. Again, including the B-matrix and D_{16} and D_{26} causes lower predicted plate strength.
- The ply region degradation model I gives slightly (0% - 5%) higher results than the complete ply degradation model I. The reason is similar to that for case A.
- The ply region degradation model II gives slightly (0% - 4%) lower values than the ply region degradation model I. For some cases, the ultimate strength is reached when all regions in a ply or all plies have failed and symmetry of the material properties has been restored. This brings the ply region degradation model II results back up to about the same level as the complete ply degradation model I on average, but there is roughly ±5% scatter.
- Setting $D_{16} = D_{26} = 0$ in the ply region degradation model II has a slight but apparently random effect, while setting $B = 0$ appears to have a random effect of up to 5%.

Overall, including the B-matrix increases calculation time due to the increased number of regions/plies that have to fail before the appearance of ultimate strength. Including the B-matrix has a more significant effect on the degradation procedure than including non-zero D_{16} and D_{26}.

6.4 Comparisons with Misirlis’s Results; Use of Ply Region Degradation Model II

For the thin plates considered, analysis using the Hashin criterion combined with the ply region degradation model II predicts much lower ultimate loads than the more detailed FE model of Misirlis. This is largely due to the neglect of post-buckling effects, which are especially important for thin plates. For the thick plates, it is necessary to perform the degradation procedure many times, i.e. with many ply regions failing before the occurrence of the ultimate load. The results for these plates are more comparable to those of Misirlis, since the post-buckling behaviour has a smaller effect. However, for the thickest plates, the ultimate stresses are still 10% - 30% smaller than those of Misirlis. This can be explained by the fact that the material degradations have been applied to a large area instead of a small element in that ply. Another important factor is that a linear degradation of the material properties has been assumed in the ABAQUS progressive failure model. The instantaneous degradation model used in this paper results in too much reduction of the stiffness. This is believed to be the main reason for the underestimation of the ultimate load. In one case, the 0.1% imperfection for the case A layup, the analysis gives a lower ultimate stress ratio for the thickest plate than for the next thickest (see Fig. 6). The reason for this rather surprising result is unclear, but one possible explanation could be that the FEA solution using the linear material degradation model overestimated the ultimate strength, the possibility of which was

noted by Misirlis [19]. For both layup cases (A and B), the shapes of the graphs (see Figs. 10-11) are somewhat similar to those of Misirlis. However, the ply region degradation model II indicates an appreciably greater sensitivity to geometric imperfections. For b/t values above about 25, the results of Misirlis indicate very little dependence on the imperfection amplitude, and the differences between these and the present results are significant.

The end shortening response and the centre out-of-plane displacement of layup case A with t = 49.98 mm and 1% imperfection amplitude are shown in Fig. 8. The end shortening response is seen to be close to a straight line even after material degradation has developed. The first peak load is reached at 250 MPa, and then the load falls to 200 MPa. The second peak is reached at 280 MPa before the load falls again to 240 MPa. The third peak, which is the ultimate load, is reached at 340 MPa and results in an end shortening of 4 mm and a lateral displacement of 13 mm in the centre.

The end shortening and central out-of-plane response of layup case B with t = 32 mm and 2% imperfection amplitude are presented in Fig. 9. The end shortening follows a straight line up to a load of 120 MPa, but the central deflection shows some non-linearity. The response is more non-linear as the load is increased towards the ultimate load (150 MPa). Some small reductions of the load are observed in between these load levels, but these are not as appreciable as in case A. The end shortening and central displacement at the ultimate load are 4.5 mm and 16 mm, respectively.

6.5 Use of Tsai-Wu Failure Criterion

The results with the Tsai-Wu criterion are compared only to those with the Hashin criterion. Both failure criteria are used with the complete ply degradation model I. With the Tsai-Wu criterion, a distinction is made between three failure modes. These are fibre tensile/compressive, matrix tensile/compressive and in-plane shear failure, respectively. In contrast, in the Hashin criterion the shear failure component is associated with the matrix mode of failure. For first ply failure, both case A and B show little difference between Hashin and Tsai-Wu. For case A, the ultimate stresses predicted using the Tsai-Wu criterion are higher than those using the Hashin criterion, especially for high thicknesses with the smallest imperfection. For case B, Tsai-Wu again gives higher values than Hashin, with the following exception - there is somewhat different behaviour for small imperfections at high thickness, and in this region Tsai-Wu gives lower values than Hashin. This could be explained by the fact that for some plies, material degradation occurs because of fibre compression. According to Section 2.2, when the Tsai-Wu failure function exceeds unity, the largest value of the individual component indicates the failure mode. For this special case, the individual functions are in some cases 0.51 for fibre failure and 0.49 for matrix failure. Again, too much degradation results in an underestimated ultimate load.

7 CONCLUSIONS

A simplified approach to the estimation of the ultimate in-plane compressive loads of composite plates with initial geometric imperfections has been investigated. In its basic form the method consists of a small-deflection buckling analysis of an imperfect plate with degradation of the stiffness properties of an entire ply as soon as the stresses in that

ply have violated a given failure criterion. Simply supported square plates with various thicknesses and geometric imperfections have been analysed. The results have been compared with an advanced analysis conducted by Misirlis using fully non-linear FE analysis with a much more detailed description of ply degradation. For thin plates, as might be expected, the neglect of post-buckling effects leads to very significant underestimation of ultimate loads. For the thicker plates considered, the simplified method gives appreciably better estimates, but they are still rather conservative. A slightly more detailed analysis in which the plate is divided into nine roughly equal regions and the stiffness degradation is limited to a single region of a failed ply gives only marginally better results, within the limitations of the implementation used so far. To improve the results significantly it will be necessary to use a large-deflection formulation; this is likely also to reveal clearer differences between the models presented in the present paper. Planned future work will include post-buckling effects and use the ply region degradation model II. This model can be expected to give appreciably better results. To improve further the agreement with Misirlis's results, a linear degradation model should be established, but, as reported in [19], this approach may actually overestimate the ultimate strength.

REFERENCES

[1] Agarwal BD, Broutman LJ, Chandrashekhara K. Analysis and performance of fiber composites. 3rd ed. USA: Wiley; 2006.

[2] Reddy JN. Mechanics of laminated composite plates and shells. 2nd ed. USA: CRC Press; 2004.

[3] Turvey GJ, Marshall IM. Buckling and postbuckling of composite plates, 1st ed. UK: Chapman & Hall; 1995.

[4] Brubak L, Hellesland J, Steen E. Semi-analytical buckling strength analysis of plates with arbitrary stiffener arrangements. J Constr Steel Res 2007; 63(4):532-543.

[5] Brubak L, Hellesland J. Approximate buckling strength analysis of arbitrarily stiffened, stepped plates. Eng Struct 2007;29(9):2321-2333.

[6] Brubak L, Hellesland J. Semi-analytical postbuckling and strength analysis of brbitrarily stiffened plates in local and global bending. Thin-Walled Struct 2007;45(6):620-633.

[7] Brubak L, Hellesland J. Strength criteria in semi-analytical, large deflection analysis of stiffened plates in local and global bending. Thin-walled Struct 2008;46(12):1382-1390.

[8] Brubak L, Hellesland J. Semi-analytical postbuckling analysis of stiffened imperfect plates with a free or stiffened edge, Comput Struct 2011;89(17-18):1574-1585.

[9] Al-Qablan H, Dwairi H, Shatarat N, Rosan T, Al-Qablan T. Stability analysis of composite panels with stiffeners and circular cutouts. Jordan J Civ Eng 2010;4(2):119-131.

[10] Al-Qablan H. Semi-analytical buckling analysis of stiffened sandwich plates. J Appl Sci 2010;10(23):2978-2988.

[11] Hayman B, Berggreen C, Lundsgaard-Larsen C, Delarche A, Toftegaard H, Dow RS, Downes J, Misirlis K, Tsouvalis N, Douka C. Studies of the buckling of composite plates in compression. Ships Offshore Struct 2011;6(1-2):81-92.

[12] Hashin Z, Rotem A. A fatigue failure criterion for fiber reinforced materials. J Compos Mater 1973;7:448-464.

[13] Misirlis K, Downes J, Dow RS. Comparison of progressive failure models for composite materials. In: Proceedings of the 10th International Conference on Fast Sea Transportation (FAST 2009). Athens: Greece; 2009.

[14] Tsai SW, Wu EM. A general theory of strength for anisotropic materials. J Compos Mater 1971;5:58-80.

[15] Knight NF. User-defined material model for progressive failure analysis. NASA Report No. NASA/CR-2006-214526. USA: NASA; 2006.

[16] Offshore standard DNV-OS-C501 composite components. Norway: Det Norske Veritas; 2003.

[17] Matzenmiller A, Lubliner J, Taylor RL. A constitutive model for anisotropic damage in fiber-composites. Mech Mater 1995;20(2):125-152.

[18] Zenkert D, Battley M. Foundations of fibre composites. KTH Report No. 96-10. Sweden: Royal Institute of Technology (KTH); 1996.

[19] Misirlis K. Progressive collapse analysis of composite ship hull sections. PhD Thesis. Newcastle: Newcastle University; 2012.

APPENDIX A: TABULATED RESULTS

Table A.1
Complete ply degradation model I: Case A (triaxial layups) with Hashin criterion.

Imp. % of b	t (mm)	No. of plies	FPF σ_{FPF} (MPa)	FPF Ply no. (direction)	"LPF" σ_{max} (MPa)	"LPF" No. of failed plies	"LPF" Ply no. (direction)	σ_{max} from [11] (MPa)	$\frac{\sigma_{max}}{\sigma_{max}[11]}$
0.1	10.02	18	31.45	18 (-45°)	31.45	1	18 (-45°)	130	0.24
0.1	16.70	18	82.83	16 (0°)	82.83	1	16 (0°)	180	0.46
0.1	24.94	18	170.81	16 (0°)	170.81	1	16 (0°)	240	0.71
0.1	33.40	18	277.70	16 (0°)	277.70	1	16 (0°)	320	0.87
0.1	49.98	18	380.79	1 (-45°)	482.69	18	3 (0°)	570	0.85
1.0	10.02	18	19.46	18 (-45°)	22.64	13	3 (0°)	130	0.17
1.0	16.70	18	43.41	16 (0°)	58.13	13	3 (0°)	180	0.32
1.0	24.94	18	74.68	16 (0°)	118.60	12	3 (0°)	235	0.50
1.0	33.40	18	106.59	16 (0°)	194.64	12	3 (0°)	300	0.65
1.0	49.98	18	165.07	16 (0°)	335.93	18	3 (0°)	435	0.77
2.0	10.02	18	13.42	18 (-45°)	20.27	13	3 (0°)	130	0.16
2.0	16.70	18	28.08	18 (-45°)	49.28	13	3 (0°)	178	0.28
2.0	24.94	18	46.71	16 (0°)	95.75	17	6 (0°)	225	0.43
2.0	33.40	18	64.91	16 (0°)	155.87	17	1&18 (-45°)	280	0.56
2.0	49.98	18	98.44	16 (0°)	280.61	18	3 (0°)	395	0.71
3.0	10.02	18	10.19	18 (-45°)	18.34	13	3 (0°)	130	0.14
3.0	16.70	18	20.15	18 (-45°)	42.99	17	1&18 (-45°)	174	0.25
3.0	24.94	18	34.08	16 (0°)	85.89	17	1&18 (-45°)	218	0.39
3.0	33.40	18	46.77	16 (0°)	137.96	17	1&18 (-45°)	260	0.53
3.0	49.98	18	70.43	16 (0°)	244.00	18	3 (0°)	360	0.68

Table A.2
Complete ply degradation model I: Case B (quadriaxial layups) with Hashin criterion.

Imp. % of b	t (mm)	No. of plies	FPF σ_{FPF} (MPa)	FPF Ply no. (direction)	"LPF" σ_{max} (MPa)	"LPF" No. of failed plies	"LPF" Ply no. (direction)	σ_{max} from [11] (MPa)	$\frac{\sigma_{max}}{\sigma_{max}[11]}$
0.1	8.00	8	21.11	8 (0°)	21.11	1	8 (0°)	105	0.20
0.1	16.00	16	80.69	16 (0°)	80.69	1	16 (0°)	180	0.45
0.1	24.00	24	166.44	24 (0°)	168.90	2	3 (90°)	215	0.79
0.1	32.00	32	197.80	3 (90°)	239.28	29	1 (0°)	270	0.89
0.1	48.00	48	203.90	3 (90°)	298.82	37	1 (0°)	340	0.88
1.0	8.00	8	14.09	8 (0°)	15.50	3	2 (+45°)	107	0.15
1.0	16.00	16	40.03	16 (0°)	57.70	5	2 (+45°)	181	0.32
1.0	24.00	24	67.90	24 (0°)	116.50	12	22 (90°)	210	0.55
1.0	32.00	32	95.20	32 (0°)	177.81	29	1 (0°)	240	0.74
1.0	48.00	48	145.15	48 (0°)	245.00	42	1 (0°)	302	0.81
2.0	8.00	8	10.31	8 (0°)	13.80	5	1 (0°)	108	0.13
2.0	16.00	16	25.97	16 (0°)	49.47	13	1 (0°)	181	0.27

2.0	24.00	24	41.85	24 (0°)	100.50	18	1 (0°)	205	0.49
2.0	32.00	32	57.34	32 (0°)	152.59	31	9 (0°)	230	0.66
2.0	48.00	48	86.65	48 (0°)	210.83	43	1 (0°)	270	0.78
3.0	8.00	8	8.14	8 (0°)	12.61	5	1 (0°)	115	0.11
3.0	16.00	16	19.25	16 (0°)	45.98	13	1 (0°)	185	0.25
3.0	24.00	24	30.32	24 (0°)	90.42	18	1 (0°)	205	0.44
3.0	32.00	32	41.20	32 (0°)	133.50	29	5 (0°)	222	0.60
3.0	48.00	48	62.00	48 (0°)	190.00	43	1 (0°)	260	0.73

Table A.3
Complete ply degradation model I: Case A (triaxial layups) with Tsai-Wu criterion.

Imp. % of b	t (mm)	No. of plies	FPF		"LPF"			σ_{max} from Table A.1 (MPa)	$\frac{\sigma_{max}}{\sigma_{max,Table\ A.1}}$
			σ_{FPF} (MPa)	Ply no. (direction)	σ_{max} (MPa)	No. of failed plies	Ply no. (direction)		
0.1	10.02	18	31.50	18 (-45°)	31.50	1	18 (-45°)	31.45	1.00
0.1	16.70	18	82.68	16 (0°)	82.68	1	16 (0°)	82.83	1.00
0.1	24.94	18	168.24	16 (0°)	168.28	2	13 (0°)	170.81	0.99
0.1	33.40	18	263.17	16 (0°)	292.20	5	1 (-45°)	277.70	1.05
0.1	49.98	18	392.76	16 (0°)	523.10	18	3&6 (0°)	482.69	1.08
1.0	10.02	18	19.65	18 (-45°)	25.15	13	3 (0°)	22.64	1.11
1.0	16.70	18	43.56	16 (0°)	64.80	13	3 (0°)	58.13	1.11
1.0	24.94	18	74.17	16 (0°)	131.11	12	3 (0°)	118.60	1.11
1.0	33.40	18	104.40	16 (0°)	209.43	11	10 (-45°)	194.64	1.08
1.0	49.98	18	156.06	16 (0°)	353.54	18	3 (0°)	335.93	1.05
2.0	10.02	18	13.62	18 (-45°)	22.75	13	3 (0°)	20.27	1.12
2.0	16.70	18	28.53	18 (-45°)	55.72	13	3 (0°)	49.28	1.13
2.0	24.94	18	46.91	16 (0°)	107.14	13	3 (0°)	95.75	1.12
2.0	33.40	18	64.67	16 (0°)	165.12	11	3 (0°)	155.87	1.06
2.0	49.98	18	96.44	16 (0°)	278.11	15	1&18(-45°)	280.61	0.99
3.0	10.02	18	10.37	18 (-45°)	20.74	13	7 (-45°)	18.34	1.13
3.0	16.70	18	20.54	18 (-45°)	48.92	13	3 (0°)	42.99	1.14
3.0	24.94	18	34.36	16 (0°)	90.74	13	3 (0°)	85.89	1.06
3.0	33.40	18	47.00	16 (0°)	139.22	17	6 (0°)	137.96	1.01
3.0	49.98	18	69.93	16 (0°)	241.88	15	1&18(-45°)	244.00	0.99

Table A.4
Complete ply degradation model I: Case B (quadriaxial layups) with Tsai-Wu criterion.

Imp. % of b	t (mm)	No. of plies	FPF		"LPF"			σ_{max} from Table A.2 (MPa)	$\frac{\sigma_{max}}{\sigma_{max,Table\ A.2}}$
			σ_{FPF} (MPa)	Ply no. (direction)	σ_{max} (MPa)	No. of failed plies	Ply no. (direction)		
0.1	8.00	8	21.12	8 (0°)	21.12	1	8 (0°)	21.11	1.00
0.1	16.00	16	80.10	16 (0°)	82.72	3	15 (+45°)	80.69	1.03
0.1	24.00	24	158.60	24 (0°)	181.27	7	22 (90°)	168.90	1.07
0.1	32.00	32	192.23	3 (90°)	256.63	14	31 (+45°)	239.28	1.07
0.1	48.00	48	196.95	3 (90°)	275.73	13	2 (+45°)	298.82	0.92

1.0	8.00	8	14.18	8 (0°)	16.68	5	1 (0°)	15.50	1.08
1.0	16.00	16	39.88	16 (0°)	60.75	7	4 (-45°)	57.70	1.05
1.0	24.00	24	66.21	24 (0°)	127.67	10	4 (-45°)	116.50	1.10
1.0	32.00	32	90.31	32 (0°)	194.38	19	27 (+45°)	177.81	1.09
1.0	48.00	48	129.79	48 (0°)	236.71	38	16 (-45°)	245.00	0.97
2.0	8.00	8	10.42	8 (0°)	15.24	5	1 (0°)	13.80	1.10
2.0	16.00	16	26.08	16 (0°)	51.63	9	3 (90°)	49.47	1.04
2.0	24.00	24	41.54	24 (0°)	103.29	18	1 (0°)	100.50	1.03
2.0	32.00	32	56.20	32 (0°)	160.47	24	26 (90°)	152.59	1.05
2.0	48.00	48	82.31	48 (0°)	225.63	48	12 (-45°)	210.83	1.07
3.0	8.00	8	8.25	8 (0°)	14.04	5	1 (0°)	12.61	1.11
3.0	16.00	16	19.41	16 (0°)	46.36	12	12 (0°)	45.98	1.01
3.0	24.00	24	30.40	24 (0°)	92.71	18	7&18(90°)	90.42	1.03
3.0	32.00	32	40.90	32 (0°)	141.16	22	1 (0°)	133.50	1.06
3.0	48.00	48	60.31	48 (0°)	194.52	31	1 (0°)	190.00	1.02

Table A.5
Complete ply degradation model II: Case A (triaxial layups) with Hashin criterion.

Imp. % of b	t (mm)	No. of plies	FPF		"LPF"			σ_{max} from Table A.1 (MPa)	$\frac{\sigma_{max}}{\sigma_{max,\text{Table A.1}}}$
			σ_{FPF} (MPa)	Ply no. (direction)	σ_{max} (MPa)	No. of failed plies	Ply no. (direction)		
0.1	10.02	18	31.45	18 (-45°)	31.45	1	18 (-45°)	31.45	1.00
0.1	24.94	18	170.81	16 (0°)	170.81	1	16 (0°)	170.81	1.00
0.1	49.98	18	381.40	1 (-45°)	430.80	18	3 (0°)	482.69	0.89
1.0	10.02	18	19.46	18 (-45°)	20.83	15	3 (0°)	22.64	0.92
1.0	24.94	18	74.68	16 (0°)	105.63	18	9 (0°)	118.60	0.89
1.0	49.98	18	165.07	16 (0°)	335.98	18	3 (0°)	335.93	1.00
3.0	10.02	18	10.20	18 (-45°)	17.01	17	18 (-45°)	18.34	0.93
3.0	24.94	18	34.08	16 (0°)	85.83	17	18 (-45°)	85.89	1.00
3.0	49.98	18	70.65	16 (0°)	243.98	18	3 (0°)	244.00	1.00

Table A.6
Complete ply degradation model II: Case B (quadriaxial layups) with Hashin criterion.

Imp. % of b	t (mm)	No. of plies	FPF		"LPF"			σ_{max} from Table A.2 (MPa)	$\frac{\sigma_{max}}{\sigma_{max,\text{Table A.2}}}$
			σ_{FPF} (MPa)	Ply no. (direction)	σ_{max} (MPa)	No. of failed plies	Ply no. (direction)		
0.1	8.00	8	20.94	8 (0°)	20.94	1	8 (0°)	21.11	0.99
0.1	24.00	24	166.28	24 (0°)	167.71	2	20 (0°)	168.90	0.99
0.1	48.00	48	204.43	3 (90°)	298.88	37	1 (0°)	298.82	1.00
1.0	8.00	8	13.91	8 (0°)	15.48	4	2 (+45°)	15.50	1.00
1.0	24.00	24	67.71	24 (0°)	113.67	19	1 (0°)	116.50	0.98
1.0	48.00	48	145.18	48 (0°)	244.79	43	1 (0°)	245.00	1.00
3.0	8.00	8	8.00	8 (0°)	11.79	4	2 (+45°)	12.61	0.93
3.0	24.00	24	30.34	24 (0°)	89.84	18	1 (0°)	90.42	0.99
3.0	48.00	48	62.17	48 (0°)	187.5	44	1 (0°)	190.00	0.99

Table A.7
Ply region degradation model I: Case A (triaxial layups) with Hashin criterion.

Imp. % of b	t (mm)	No. of plies	FPF		"LPF"		σ_{max} from Table A.1 (MPa)	$\frac{\sigma_{max}}{\sigma_{max,Table\ A.1}}$
			σ_{FPF} (MPa)	Ply no. (direction)	σ_{max} (MPa)	Ply no. (direction)		
0.1	10.02	18	31.45	18 (-45°)	31.45	18 (-45°)	31.45	1.00
0.1	24.94	18	170.81	16 (0°)	170.81	16 (0°)	170.81	1.00
0.1	49.98	18	380.79	1 (45°)	482.69	3 (0°)	482.69	1.00
1	10.02	18	19.46	18 (-45°)	22.95	3 (0°)	22.64	1.014
1	24.94	18	74.68	16 (0°)	119.89	3 (0°)	118.60	1.011
1	49.98	18	165.07	16 (0°)	335.93	3 (0°)	335.93	1.00

Table A.8
Ply region degradation model I: Case B (quadriaxial layups) with Hashin criterion.

Imp. % of b	t (mm)	No. of plies	FPF		"LPF"		σ_{max} from Table A.2 (MPa)	$\frac{\sigma_{max}}{\sigma_{max,Table\ A.2}}$
			σ_{FPF} (MPa)	Ply no. (direction)	σ_{max} (MPa)	Ply no. (direction)		
0.1	8.00	8	21.11	8 (0°)	21.11	8 (0°)	21.11	1.00
0.1	24.00	24	166.44	24 (0°)	172.08	3 (90°)	168.90	1.019
0.1	48.00	48	203.90	3 (90°)	298.82	1 (0°)	298.82	1.00
1	8.00	8	14.09	8 (0°)	16.25	6 (90°)	15.50	1.048
1	24.00	24	67.90	24 (0°)	119.17	1 (0°)	116.50	1.023
1	48.00	48	145.15	48 (0°)	245.00	1 (0°)	245.00	1.00

Table A.9
Ply region degradation model II: Case A (triaxial layups) with Hashin criterion.

Imp. % of b	t (mm)	No. of plies (no. of ply regions)	FPF		"LPF"			σ_{max} from [11] (MPa)	$\frac{\sigma_{max}}{\sigma_{max}[11]}$
			σ_{FPF} (MPa)	Ply no. (direction)	σ_{max} (MPa)	No. of matrix failed ply regions	No. of fibre failed ply regions		
0.1	10.02	34 (306)	31.19	32 (0°)	31.19	1	0	130	0.24
0.1	16.70	34 (306)	81.59	32 (0°)	81.59	1	0	180	0.45
0.1	24.94	34 (306)	167.03	32 (0°)	167.03	1	0	240	0.70
0.1	33.40	34 (306)	269.84	32 (0°)	269.84	1	0	320	0.84
0.1	49.98	34 (306)	381.40	1 (-45°)	431.42	306	1	570	0.76
1.0	10.02	34 (306)	19.02	32 (0°)	21.21	172	0	130	0.16
1.0	16.70	34 (306)	40.42	32 (0°)	51.74	166	0	180	0.29
1.0	24.94	34 (306)	68.66	32 (0°)	106.94	297	1	235	0.46
1.0	33.40	34 (306)	97.45	32 (0°)	179.08	291	1	300	0.60
1.0	49.98	34 (306)	150.06	32 (0°)	336.38	301	1*	435	0.77
2.0	10.02	34 (306)	13.32	32 (0°)	18.12	290	1	130	0.14
2.0	16.70	34 (306)	26.10	32 (0°)	47.06	291	7	178	0.26
2.0	24.94	34 (306)	42.10	32 (0°)	95.98	297	1	225	0.43
2.0	33.40	34 (306)	58.34	32 (0°)	155.64	296	1	280	0.56
2.0	49.98	34 (306)	88.16	32 (0°)	276.99	302	1	395	0.70

3.0	10.02	34 (306)	10.20	34 (-45°)	17.25	290	1	130	0.13
3.0	16.70	34 (306)	19.27	32 (0°)	43.81	289	1	174	0.25
3.0	24.94	34 (306)	34.45	32 (0°)	87.21	293	1	218	0.40
3.0	33.40	34 (306)	41.73	32 (0°)	138.47	296	1	260	0.53
3.0	49.98	34 (306)	62.84	32 (0°)	238.22	298	1	360	0.66

*In these ply regions fibre failure occurred without matrix failure.

Table A.10
Ply region degradation model II: Case B (quadriaxial layups) with Hashin criterion.

Imp. % of b	t (mm)	No. of plies (no. of ply regions)	FPF		"LPF"			σ_{max} from [11] (MPa)	$\frac{\sigma_{max}}{\sigma_{max}[11]}$
			σ_{FPF} (MPa)	Ply no. (direction)	σ_{max} (MPa)	No. of matrix failed ply regions	No. of fibre failed ply regions		
0.1	8.00	8 (72)	20.94	8 (0°)	20.94	1	0	105	0.20
0.1	16.00	16 (144)	80.47	16 (0°)	80.47	1	0	180	0.45
0.1	24.00	24 (216)	166.28	24 (0°)	169.14	10	0	215	0.79
0.1	32.00	32 (288)	198.24	3 (90°)	236.82	252	1*	270	0.88
0.1	48.00	48 (432)	204.43	3 (90°)	300.78	324	1*	340	0.88
1.0	8.00	8 (72)	13.91	8 (0°)	15.60	25	0	107	0.15
1.0	16.00	16 (144)	39.84	16 (0°)	61.33	48	0	181	0.34
1.0	24.00	24 (216)	67.71	24 (0°)	114.58	34	0	210	0.55
1.0	32.00	32 (288)	95.21	32 (0°)	177.25	258	0	240	0.74
1.0	48.00	48 (432)	145.18	48 (0°)	246.09	374	1*	302	0.81
2.0	8.00	8 (72)	10.16	8 (0°)	13.61	29	0	108	0.13
2.0	16.00	16 (144)	25.83	16 (0°)	51.07	59	0	181	0.28
2.0	24.00	24 (216)	41.80	24 (0°)	100.78	158	1	205	0.49
2.0	32.00	32 (288)	57.37	32 (0°)	151.37	257	1*	230	0.66
2.0	48.00	48 (432)	86.59	48 (0°)	210.94	381	1*	270	0.78
3.0	8.00	8 (72)	8.00	8 (0°)	12.11	29	0	115	0.11
3.0	16.00	16 (144)	19.14	16 (0°)	45.41	99	2	185	0.25
3.0	24.00	24 (216)	30.34	24 (0°)	90.63	158	1	205	0.44
3.0	32.00	32 (288)	41.26	32 (0°)	133.30	210	1	222	0.60
3.0	48.00	48 (432)	62.17	48 (0°)	190.76	382	1	260	0.73

*In these ply regions fibre failure occurred without matrix failure.

Table A.11
Ply region degradation model II: Test with B-matrix and D_{16} and D_{26}. Case A (triaxial layups) with Hashin criterion.

Imp. % of b	t (mm)	No. of plies (no. of ply regions)	Changes in the model	FPF	"LPF"			σ_{max} from Table A.9 (MPa)	$\frac{\sigma_{max}}{\sigma_{max,Table\ A.9}}$
				σ_{FPF} (MPa)	σ_{max} (MPa)	No. of matrix failed ply regions	No. of fibre failed ply regions		
1.0	16.70	34 (306)	$B = 0$	40.42	57.54	130	0	51.74	1.11
1.0	16.70	34 (306)	$D_{16} = D_{26} = 0$	40.42	51.46	166	0	51.74	0.99
3.0	16.70	34 (306)	$B = 0$	19.27	43.79	251	4	43.81	1.00
3.0	16.70	34 (306)	$D_{16} = D_{26} = 0$	19.27	43.79	289	1	43.81	1.00
1.0	33.40	34 (306)	$B = 0$	97.45	188.44	136	0	179.08	1.05

1.0	33.40	34 (306)	$D_{16} = D_{26} = 0$	97.45	177.67	296	1	179.08	0.99
3.0	33.40	34 (306)	$B = 0$	41.73	138.10	245	1	138.47	1.00
3.0	33.40	34 (306)	$D_{16} = D_{26} = 0$	41.73	138.47	296	1	138.47	1.00

Table A.12
Ply region degradation model II: Test with B-matrix and D_{16} and D_{26}. Case B (quadriaxial layups) with Hashin criterion.

Imp. % of b	t (mm)	No. of plies (no. of ply regions)	Changes in the model	FPF	"LPF"			σ_{max} from Table A.10 (MPa)	$\frac{\sigma_{max}}{\sigma_{max,\text{Table A.10}}}$
				σ_{FPF} (MPa)	σ_{max} (MPa)	No. of matrix failed ply regions	No. of fibre failed ply regions		
1.0	16.00	16 (144)	$B = 0$	39.84	59.96	44	0	61.33	0.98
1.0	16.00	16 (144)	$D_{16} = D_{26} = 0$	40.04	62.40	57	0	61.33	1.02
3.0	16.00	16 (144)	$B = 0$	19.14	44.92	97	0	45.41	0.99
3.0	16.00	16 (144)	$D_{16} = D_{26} = 0$	19.24	46.88	99	0	45.41	1.03
1.0	48.00	48 (432)	$B = 0$	145.18	246.09	369	1*	246.09	1.00
1.0	48.00	48 (432)	$D_{16} = D_{26} = 0$	145.18	246.09	374	1*	246.09	1.00
3.0	48.00	48 (432)	$B = 0$	62.17	200.52	385	3	190.76	1.05
3.0	48.00	48 (432)	$D_{16} = D_{26} = 0$	62.17	187.50	380	1	190.76	0.98

*In these ply regions fibre failure occurred without matrix failure.